Influence of the structural non–linearity on the performance o fan electret–based vibration energy harvester

7th ECCOMAS Thematic Conference on Smart Structures and Materials
SMART 2015
A.L. Araújo, C.A. Mota Soares, et al. (Editors)

INFLUENCE OF THE STRUCTURAL NON–LINEARITY ON THE PERFORMANCE OF AN ELECTRET–BASED VIBRATION ENERGY HARVESTER

Eugenio G.M. Brusa[†], Mircea Gh. Munteanu[*]

[†]Dept. Mechanical and Aerospace Engineering, Politecnico di Torino
Corso Duca degli Abruzzi, 24 – 10129 Torino, Italy
eugenio.brusa@polito.it

[*]Dept. Electrical, Managerial, Mechanical Engineering, Università degli Studi di Udine
Via delle Scienze, 208 – 33100 Udine, Italy
mircea.munteanu@uniud.it

Key words: Electret material, Vibration Energy Harvester, Finite Element Method, Nonlinear dynamics.

Summary: *Films of electret material are currently used to cover the surface of electrodes of some vibration capacitive harvesters based on deformable beams, clamped at both ends. Nevertheless, performance of this device is often predicted through some simplified electromechanical model, which neglects the effect of geometric nonlinearity due to a mechanical coupling between the axial and flexural behaviors of the clamped beam. Stiffening of beam and nonlinear behavior are herein investigated, by resorting to a distributed model of electromechanical coupling of the vibration harvester, based on the finite element method. Influence upon the performance of energy conversion is then analyzed and an optimization of the configuration is proposed to assess some suitable design criteria.*

1 INTRODUCTION

Use of electret materials in microsystems is currently proposed to improve some features of miniaturized smart devices and to increase the availability of autonomous power supplies. It is known that electrets might exhibit an internal polarization due to either a set of trapped charges, in the so–called non–polar space–charge configuration, or to some oriented molecular dipoles in polar electrets, although it is even possible a combination of those two effects [1]. Behavior of these materials is very close to some polar piezoelectric polymer like polyvinylidene fluoride (PVDF), in which the piezoelectric effect basically is due to a change of dipole density under either mechanical stress or electric field. New non–polar electrets exhibit a charge separation which is associated to void surfaces, being oppositely charged. Mechanical stress leads to decrease the void size and this effect allows to generate an electric voltage. Therefore, electrets exhibit a fairly good electromechanical coupling, if they are suitably charged, during their preparation. Pyroelectricity of electrets is approximately a couple of orders of magnitude lower than in classical piezoelectric materials such as PVDF. Another property concerns the electrical resonance, being in the high range of kHz up to the

low MHz region. This peculiarity makes electrets material suitable for application to microphones and loudspeakers, with a low distortion. Electrets look less effective in terms of thermal stability, since at higher temperature polarization decreases. Structural properties of electrets allow their application as sensors and actuators in material testing and in industrial gas–flow measurements, but an increasing use within MEMS is observed. Piezoelectric coupling coefficients are fairly high, while inertia associated to the thin film is usually less than in piezoceramics. High resistance and thinness makes electrets candidate for manufacturing thin switches and digital keypads, because of their nature of functional membrane being compatible with tactile devices with an appreciated mechanical reliability [2]. Those properties motivate the application as a tactile sensor, but evenly as a part of MEMS capacitive energy harvester.

Vibration energy harvesters are nowadays used in some applications to convert kinematic energy into electric charge, especially when it is required that device is sufficiently small and easily wearable, as in case of human health care and monitoring. Sometimes small size is required to use this device in industrial components, machines and vehicles [3]. In practice, a sort of local power supply is built up for miniaturized and autonomous systems. In case of electrostatic capacitive harvester it is required an electric pre–charging to provide a bias voltage to operate [4]. This limit can be overcome by using a thin layer of electrets material, which might be positioned within the dielectric of capacitor to play the role of constant voltage generator. Electromechanical damping force depends on bias voltage, therefore this pre–charging allows optimizing the dynamic behavior of vibration energy harvester.

An electrostatic generator based on electrets was proposed in [5] and it was built up by placing the electret layer in parallel with two variable comb drive capacitors operating in anti–phase, thus resulting in a charge transfer between variable capacitors as proof mass moves. Nevertheless, the same authors optimized the application to one variable capacitor, thus moving the industrial interest towards this configuration, as in [6], where an electret with variable air gap is used.

A clear discussion about performance of vibration energy harvesters based on a capacitive transducer equipped with an electret layer was provided in [7]. The authors performed a comparison of efficiency among piezoceramics, electrets based and electromagnetic systems. Conclusion was that if electrets are surface bonded on a moveable plate of capacitor and it moves over the fixed electrode at a almost constant gap, benefit of electric charging is higher in electrets–based system than in the electromagnetic device. In practice, if the system is small and relative speed fairly low, electrostatic coupling may offer a higher resistivity and a lower dissipation, although electromagnetic coupling is better for higher impedances. This comparison shows that efficiency is strictly dependent on the scale of system and is rather difficult to define a clear dominant solution between the two above mentioned. When piezoelectric effect is compared to a variable gap capacitor which is equipped with an embedded electret layer, it is clear that coupling coefficients are fairly different and piezoceramic material looks stronger. Nevertheless piezoelectric is stiffer, heavier and potentially prone to crack. An application in which the electrets–based vibration energy harvesters are preferred could be those in which the device is required to be fairly small, light, soft and reliable [4].

This screening suggests that a prediction of the overall performance of electret materials for MEMS should be based on a detailed modeling of electromechanical coupling and effects of structural compliance should be analyzed, especially in case of structural nonlinearity.

2 GOALS OF INVESTIGATION

2.1 State of the arts in design of electrets–based vibration energy harvester

Modeling of capacitive microsystems based on electrets materials is very often performed in the literature by resorting to the simple model of plane capacitors with multiple layers as in case of ductile or gas sensors [8] or of small actuators [9]. When a rotating and floating layer is used to create the electrostatic coupling, modeling activity is quite simple and follows a fairly traditional approach, based on some discrete mathematical models [4]. In case of variable gap capacitor with embedded electrets the same modeling activity can be applied if electrodes behave like almost rigid bodies, in this case very often an equivalent voltage generator is used to represent the electrets effects [10]. When flexible electrodes are considered to convert energy associated to vibration, like in case of a beam clamped to both its ends, electromechanical coupling is distributed upon the surface of electrodes and might be affected by phenomena like the axial–flexural coupling of the deformable electrode, as in [11]. In this case electromechanical stability, pull–in phenomenon, charge distribution are considerably linked to the structural behavior of the flexible structure, when the electret is fixed to wafer. Moreover, it could be considered as a part of the deformable structure, if it is bonded on the structure surface [12].

This paper proposes a detailed analysis of distributed voltage and loading condition upon a double clamped flexible vibration energy harvester with embedded electrets. Performance will be compared to that predicted by discrete models as in [12]. Nonlinearities associated to the electromechanical coupled behavior will be then analyzed and compared to some previous papers like [13], where dynamic behavior of the energy harvester was analyzed in the frequency domain. Moreover, effects of nonlinear dynamics will be even compared to [14] where nonlinear spring elements were just introduced to suspend the moveable electrode.

According to the numerical investigation herein performed it will be described how the system configuration can be assessed to get the highest performance from this device by suitably using its nonlinear characteristic behavior and the flexibility of supports.

2.2 Configurations of electrets–based vibration energy harvester

Configuration of the electrets–based vibration energy harvester looks like in Fig.1, when a unique compliant element is applied to the moveable electrode to allow the in–plane and out –of–plane oscillation, respectively [15]. In some application vibration excites the in–plane oscillation of this device, thus making variable over time the area of moveable electrode actually faced to the fixed one. In other cases vibration excites vertical displacement, thus inducing a variability of gap over time. Both those parameters are affecting the value of capacitance. In many models a unique source of nonlinearity in this configuration is the electromechanical force applied between electrodes, being nonlinearly depending on voltage charge and gap [16]. Moveable electrode is assumed to be perfectly rigid. Very often relation between force and displacement in compliant connectors, i.e. of lateral springs in Fig.1, is assumed to be linear. This configuration very seldom corresponds and effectively describes the real system. To reduce the structural stiffness and to calibrate the resonance of the energy harvester the cantilever–based configuration of Fig.2 is applied. It resorts to a cantilever beam to have a compliant element, being sensitive to vibration. In this case excitation is basically applied along the vertical direction, through the clamp [12]. To limit the rotation of tip mass when beam is bended and to control better the relative position of electrodes a

configuration with both the beam ends clamped is proposed, as in [13], and looks like in Fig.3.

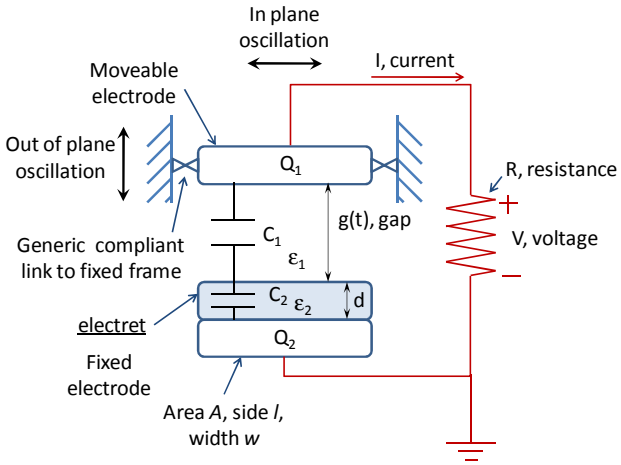

Figure 1: Discrete model of the electrets–based vibration energy harvester.

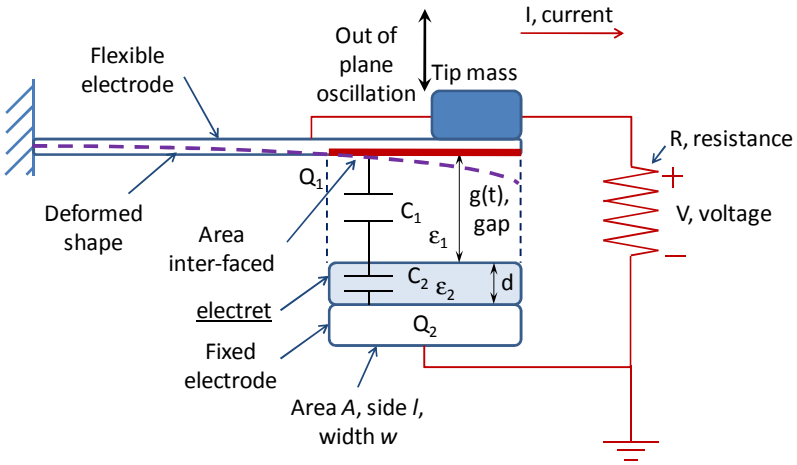

Figure 2: Electrets–based vibration energy harvester with cantilever flexible electrode.

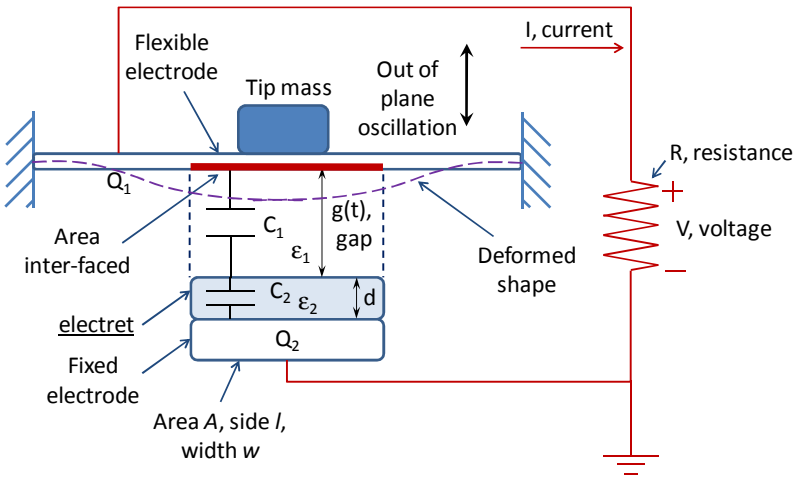

Figure 3: Electrets–based vibration energy harvester with clamped–clamped beamlike electrode.

It is important noticing that constraints of Fig.2 and Fig.3 are very different in terms of structural behavior. Beam in Fig.2 is statically and kinematically determinate, i.e. number of degrees of freedom of the beam solid and number of degrees of freedom inhibited by the clamp are equal and no motion of tip mass is allowed without deforming the beam. System in Fig.3 is kinematically determinate, i.e. only a deformation of beam allows displacing the tip mass bonded on its surface, but it is statically indeterminate since the number of degrees of freedom inhibited by constraints is larger than that of beam, seen as a rigid body. Benefit of such configuration is that mass tends to move by keeping its lower face plane and better interfaced to lower electrode, thus inducing a regular distribution of voltage through the gap and of charge upon surfaces. Nevertheless, it is a sort of over–constrained configuration, where equilibrium in static and dynamic behavior strictly depends on the deformed shape. In particular, when displacement of tip mass is sufficiently large the material of beam is highly stretched by clamps, because of a mechanical coupling between the flexural behavior of beam with its axial behavior. It happens that as the tip mass induces a larger displacement of the cross section of beam, reactions of clamps grow up and axial loading effect increases, thus stiffening the structure.

2.3 Purpose of this study

As above mentioned three configurations are mainly proposed in the literature to evaluate the effectiveness of electrets–based vibration energy harvester. Provided that electrets exhibit an electromechanical coupling effect weaker than other smart materials like piezoelectrics, possibility of embedding electrets layers into capacitive energy harvesters could motivate their use in some application. Therefore, goal of this paper is investigating:

- nonlinear dynamic effects in harvester operation to be included in models;
- influence of nonlinear behavior of beam structure on the performance of the energy harvester, i.e. on power conversion being associated to maximum displacement of tip mass and to frequency range in which the device could effectively operate;
- criteria which might be applied in design activity to eventually exploit nonlinear behavior to enhance the system performance.

As a main test case configuration described in Fig.3 will be analyzed, as it looks in the graphical impression of Fig.4.

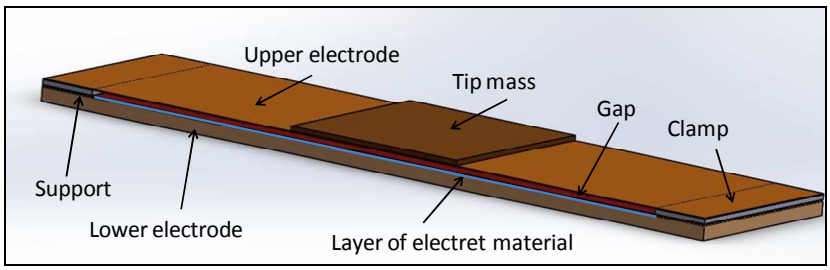

Figure 4: Investigated configuration of electrets–based vibration energy harvester

3 ANALYSIS

3.1 Basic model of electrets–based vibration energy harvester

To appreciate some critical issues of configuration depicted in Fig.4 a basic model of electromechanical coupling usually proposed in the literature is here described. According to

Fig.3 if coordinate ξ is the instantaneous distance between the lower surface of flexible electrode and the upper surface of electrets layer, in a simplified model with a single mechanical degree of freedom, dynamic equilibrium of electromechanically coupled and damped system is [12]:

$$m\ddot{\xi} + b\dot{\xi} + k\xi = -m\ddot{\eta} + F_e \qquad F_e = \frac{1}{2}\frac{Q_1^2(t)}{A\varepsilon_0\varepsilon_1} \tag{1}$$

being m the tip mass, b damping applied to system, k structural stiffness, η coordinate representative of vibration applied to clamps in the fixed reference frame, ε_1 relative permittivity of dielectric, ε_0 that of vacuum, A the surface area of interfaced electrodes and t the time.

The equivalent circuit is corresponding to description of Fig.5. Electret material supplies a constant and bias voltage, V_2, by an increment of electric charge, between the lower electrode where charge is Q_2 and the upper one where, in this case and because of embedded layer of electrets, charge is Q_1. Capacitance C_2 and voltage V_2 of electret material are almost constant, apart from degradation of polarization properties induced by temperature or aging [2]. Power converted, P, can be measured through a resistive load, R, as a product of voltage, V, and current I. Those two variables can be related to the energy harvester parameters as follows :

$$\begin{aligned}
&V_2 = V_1 + V; \quad V = V_2 - V_1; \quad V_1 = \frac{Q_1}{C(t)}; \quad V_2 = const.\\
&C(t) = \frac{C_1 C_2}{C_1 + C_2}; \quad C_1 = \frac{A\varepsilon_0\varepsilon_1}{\xi(t)}; \quad C_2 = const.\\
&P(t) = RI^2(t) = R\left(C(t)\frac{dV}{dt}\right)^2 = R\left(\frac{dQ_1}{dt}\right)^2;\\
&P(t) = R\left[\frac{V_2^2}{R} - \frac{Q_1\left(\frac{A\varepsilon_0\varepsilon_1}{\xi(t)} + C_2\right)}{\frac{A\varepsilon_0\varepsilon_1}{\xi(t)}C_2}\right]^2
\end{aligned} \tag{2}$$

Actually total capacitance C is a result of the series of two capacitances depicted in Fig.3, namely C_1 and C_2. The first one is depending on the relative position of electrodes, ξ, as well as electromechanical force F_e depends on electric charge Q_1. This relations define the coupling between mechanical and electric behaviors.

Model of the electromechanical coupled system is therefore:

$$\begin{aligned}
&m\ddot{\xi} + b\dot{\xi} + k\xi = -m\ddot{\eta} + \frac{1}{2}\frac{Q_1^2(t)}{A\varepsilon_0\varepsilon_1}\\
&I(t) = \frac{dQ_1}{dt} = \frac{V_2}{R} - \frac{Q_1\left(\frac{A\varepsilon_0\varepsilon_1}{\xi(t)} + C_2\right)}{\frac{A\varepsilon_0\varepsilon_1}{\xi(t)}C_2 R}
\end{aligned} \tag{3}$$

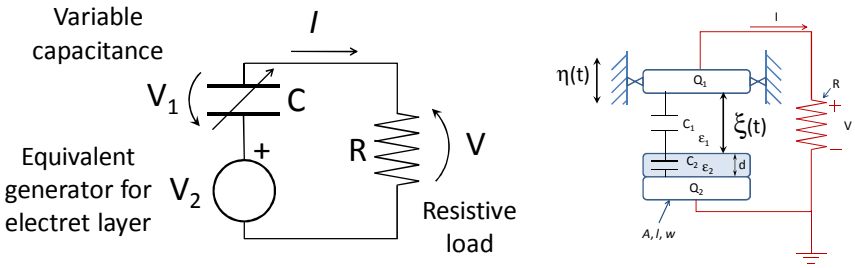

Figure 5: Equivalent circuit and simplified sketch of configuration of Fig.1

Identification of parameters in Eq.(3) is a key step of modeling and design activity. In case of cantilever–based system in the literature a simplified approach assumes that mass is corresponding strictly to tip mass, although a contribution can be given by the beam, depending on the excited vibration mode. Moreover, damping is rather difficult to be clearly evaluated if structural effect due to loss factor and air damping or squeeze film are present. A crucial point is structural stiffness, being very often simply assumed to be that of a linear static deflection of beam under a concentrated load applied to tip mass [13]. This assumption does not consider the real contribution of beam vibration mode to the dynamic response of the energy harvester, but more relevant is fact that nonlinearities due to beam stretching and to fairly large displacement of beam cross section are neglected.

3.2 Modeling of continuous beam configuration: linear approach

To investigate the nonlinear effects above mentioned test case of [12] was first considered. It looks like in Fig.2. Main properties are resumed in Table 1. As it was previously remarked, because of beam deformation in bending, gap $g(t)$ is not constant along the electret side. Local value of gap can be written as:

$$g(x,t) = g_0 - v(x,t) \tag{4}$$

where g_0 is the equilibrium condition about which vibration of electrode occurs, v is the displacement of moveable electrode from its initial shape, being measured along the portion of the line axis interfaced with the electret layer. Coordinate x runs along the line axis of beam, from the clamp to the free end. To suitably describe the variable capacitance of the device, it is required to integrate effects of variable gap as follows:

$$C(t) = \frac{1}{\frac{d}{\varepsilon_2 \varepsilon_0 A} + \frac{1}{\varepsilon_1 \varepsilon_0} \frac{1}{\int_\lambda \frac{w}{g(x,t)} dz}} \Leftrightarrow C(t) = \frac{1}{\frac{d}{\varepsilon_2 \varepsilon_0 A} + \frac{1}{\varepsilon_1 \varepsilon_0} \frac{1}{\sum_{i=1}^{n} \frac{A_i}{g(x_i,t)}}} \tag{5}$$

where λ is the length of electret layer along the x–axis. When system is discretized through the finite element approach expression of capacitance becomes the second one written in Eq.(5), where n is the number of electrical degrees of freedom of discrete model, which is based on a regular subdivision of electrode area in elementary subareas, A_i, whose middle point along the line axis is corresponding to the x_i coordinate. In some case a refinement of

discretization might suggest of resorting to *n* segments not exactly equal.

Mass	[kg]	$5\cdot10^{-3}$
Young's modulus, E	[MPa]	$1.6\cdot10^{11}$
Beam width	[m]	$1.3\cdot10^{-2}$
Beam thickness	[m]	$3\cdot10^{-4}$
Beam length	[m]	$3\cdot10^{-2}$
Voltage	[V]	1400
Resistance	[Ω]	$2.18\cdot10^{9}$
Electrect thickness, d	[m]	$1.27\cdot10^{-4}$
Initial gap, g	[m]	$5.93\cdot10^{-4}$
Interfaced length of electrode, λ	[m]	$9.6\cdot10^{-3}$
Imposed acceleration, ÿ	[m/s^2]	4
Frequency of vibration	[Hz]	51.32
Dielectric permittivity of vacuum, ε_0	[pF/μm]	$8.854\cdot10^{-6}$
Relative dielectric permittivity, ε_1		1.00059
Relative dielectric permittivity, ε_2		2.0
Length of tip mass	[m]	$4\cdot10^{-3}$

Table 1: Test case analyzed in numerical simulation.

A coupled model of continuous structure of beam can be performed by means of the finite element method (FEM) as follows:

$$\begin{aligned} &[\overline{M}]\{\ddot{v}\}+[\overline{C}]\{\dot{v}\}+[\overline{K}]\{v\}=\{\overline{F}\}-\ddot{y}_0[\overline{M}]\begin{Bmatrix}1\\ \vdots\\ 1\end{Bmatrix}-\frac{d}{d\{v\}}\left(\frac{Q^2}{2C(t)}\right) \qquad y(t)=y_0\sin(\omega\cdot t)\\ &\frac{dQ(t)}{dt}=\frac{V}{R}-\frac{Q}{C(t)R} \end{aligned} \tag{6}$$

where $\{v\}$ describes the vertical displacement of the *n* electrical degrees of freedom of moveable electrode with respect of the fixed counter–electrode, while vector $\{F\}$ includes all the mechanical actions. Structural analysis is performed by means of the first equation, but to make compatible the degrees of freedom of the mechanical and electromechanical analyses, respectively, two steps are performed. Beam is firstly discretized with two–dimensional beam elements, with two nodes and three degrees of freedom per each node (*u*, *v* and rotation). All relevant matrices are derived, as mass matrix [M], damping matrix [C], stiffness matrix [K] and mechanical actions are applied in $\{F\}$. Nevertheless, to describe the dynamic response of the cantilever beam coupled with the energy harvester it is mainly required investigating the degrees of freedom corresponding to nodes distributed along the electrode. Therefore, all the above mentioned matrices are reduced, by selecting nodes corresponding to the electrical degrees of freedom along the electrets, as master degrees. In Eq.(6) over lined symbols mean that a reduction of degrees of freedom was applied. Mass was considered to be concentrated in those nodes, thus applying a reduction somehow similar to static condensation [17]. The mass matrix looks like:

$$\left[\overline{M}\right]=\underbrace{\begin{bmatrix} m_1 & 0 & 0 \\ 0 & \ddots & 0 \\ 0 & 0 & m_n \end{bmatrix}}_{nxn} \tag{7}$$

The sum of all of partial masses m_i is equal to the total mass. Damping matrix is usually defined by resorting to assumption of proportional damping, while acceleration of all the nodes of the discretized system was assumed to be equal, i.e. only a translation motion along the vertical direction was considered, although a rotation about the clamp may be even added. Unit vector appearing in Eq.(6) includes n elements.

Electromechanical action appears on the right hand of Eq.(6) as a column of n elements:

$$\{F_{em}\}=\frac{d}{d\{v\}}\left(\frac{Q_1^2}{2C(t)}\right)\Leftrightarrow\frac{d}{dy_i}\left(\frac{Q_1^2}{2C(t)}\right)=-Q_1^2\frac{\varepsilon_0\varepsilon_1 A_i}{\left(\sum_{j=1}^{n}\frac{\varepsilon_0\varepsilon_1 A_j}{g_0-v_j(t)}\right)^2(g_0-v_i(t))^2} \tag{8}$$

where g_0 is the initial constant gap between two electrodes. The above numerical system can be written to be solved by means of the Runge–Kutta solution method as:

$$\begin{cases} \dot{Q}_1=\dfrac{V}{R}-\dfrac{Q_1}{C(t)R} \\ \{\dot{v}\}=\{z\} \\ \{\dot{z}\}=\left[\overline{M}\right]^{-1}\left(-\left[\overline{C}\right]\{z\}-\left[\overline{K}\right]\{v\}+\{F_{em}(v)\}\right)-\{\ddot{y}_0\} \end{cases} \tag{9}$$

being composed by $2n+1$ differential equations of first order. Solution can be found iteratively by updating alternately the vector of electromechanical forces F_{em} and value of capacitance C for each increment of displacement v and finding the new displaced configuration of beam tip region.

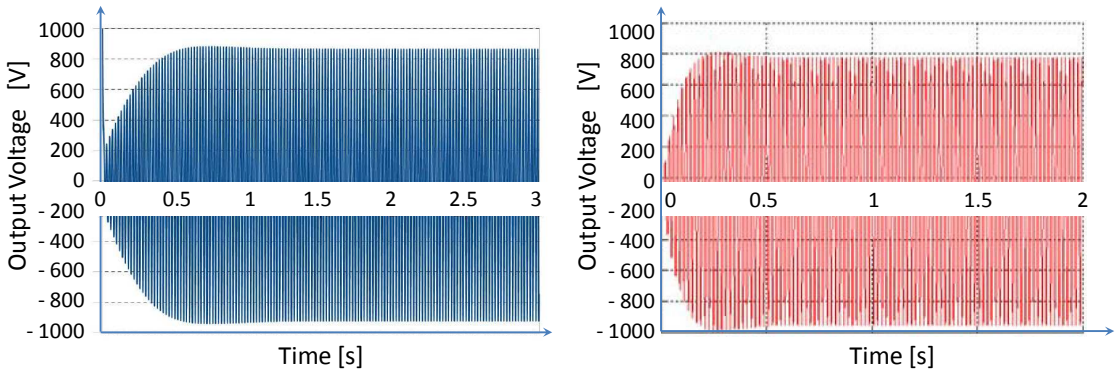

Figure 6: Comparison between results for the test case presented by [12] and results of numerical simulation based on the linear model

If numerical results obtained by using model of Eq.(9) and results described in [12], for the test case with optimized configuration, are compared it can be noticed that agreement is good (Fig.6), provided that damping coefficient was set at the same value. In that case maximum displacement of tip mass was within a range of about 2% of its length.

3.3 Modeling of continuous beam configuration: nonlinear approach

Actually model previously described assumes that stiffness of beam just corresponds to the classical definition provided in linear models. Nevertheless, already in cantilever configuration elastic forces described by product of stiffness matrix and vector of displacements might be a non constant or nonlinear contribution. It happens when conditions for the so–called geometrical nonlinearity (improperly called large displacement nonlinearity) occur. In that case it is required resorting to the second order theory of beam [11]. Difference between first order beam theory and second order can be shortly shown in following equations:

$$\begin{cases} \dfrac{d^2u}{dx^2} = 0 \\ N = EA\dfrac{du}{dx} \end{cases} \qquad \begin{cases} EI\dfrac{d^4v}{dx^4} = p \\ M = EI\dfrac{d^2v}{dx^2} \end{cases} \tag{10}$$

The above set of Eq.(10) describes the linear first order theory. It can be basically appreciated that for a linear distribution of vertical load, *p*, in linearity flexural and axial behaviors are uncoupled, thus allowing to compute the axial effort *N* separately from the bending moment *M*. Those actions are calculated by means of corresponding strains, which are directly expressed as a function of axial displacement *u* and vertical displacement *v*, but appear separately in the two above mentioned equations. Other symbols are Young's modulus of elasticity, *E*, cross section area of beam, *A*, transversal moment of area of the second order (improperly flexural inertia), *I*.

When the second order theory of beam is considered above equations become:

$$\begin{cases} \dfrac{d^2u}{dx^2} + \dfrac{dv}{dx}\dfrac{d^2v}{dx^2} = 0 \\ EI\dfrac{d^4v}{dx^4} = p + EA\dfrac{du}{dx}\dfrac{d^2v}{dx^2} \\ N = EA\left[\dfrac{du}{dx} + \dfrac{1}{2}\left(\dfrac{dv}{dx}\right)^2\right] \\ M = EI\dfrac{d^2v}{dx^2} \end{cases} \tag{11}$$

As it looks clear a coupling effect between axial and flexural behavior, respectively, occurs. Load distribution affects the axial strain of beam, while axial effort is coupled with vertical displacement, *v*. This coupling can be due in cantilever configuration to a rotation of tip sufficient to create conditions for the load to apply a component along the line axis, as it happens in Fig.2 if deflection is sufficiently large. Moreover, in case of a clamped–clamped

configuration, constraints apply an axial force to the beam under bending even when vertical displacements are small.

It is remarkable that it is not required that vertical displacement *v* is absolutley so large to induce the coupling effect. To include elements of the second order theory inside the model of Eq.(6) it is sufficient to formulate the stiffness matrix by including all the elements describing its dependance on the increasing normal effort *N*, as a function of displacement *v*. Details are described in [11].

$[K]=[K_0]+[K_{NL}]$
$[K_0] \Rightarrow$ I order theory; linear, small displacements,
axial and flexural behaviors uncoupled
$[K_{NL}] \Rightarrow$ Second order approximation theory, larger displacements,
axial and flexural behaviors coupled by a variable normal effort
N (clamped - clamped beam like Fig.3)

Table 2: Components of stiffness matrix of the beam structure

In the nonlinear case the equation (9) becomes:

$$\begin{cases} \dot{Q}_1 = \dfrac{V}{R} - \dfrac{Q_1}{C(t)R} \\ \{\dot{v}\} = \{z\} \\ \{\dot{z}\} = [\overline{M}]^{-1}\left(-[\overline{C}]\{z\} - \{F_{el}\} + \{F_{em}(v)\}\right) - \{\ddot{y}_0\} \end{cases} \tag{12}$$

where $\{F_{el}\}$ represents the vector of elastic forces that in the linear case are $\{F_{el}\} = [\overline{K}]\{v\}$. When the structural behavior is no longer linear, the elastic forces are computed using an iterative approach. In the frame of Runge–Kutta method, at each time step, displacements $\{v\}$ are known and elastic forces and electromechanical forces are accordingly computed. The elastic forces are computed iteratively following the Newton–Raphson method. The Runge–Kutta method is used to solve the differential system (12). It requires very small time steps and therefore at maximum two iterations are needed to apply the Newton–Raphson method. This approach was deeply developed within the theory of nonlinear finite elements in [17].

4 INVESTIGATION ABOUT NONLINEARITY ADVANTAGES IN DESIGN OF ELECTRETS-BASED ENERGY HARVESTER

4.1 Stiffening effect on doubly clamped structure

A practical comparison between the real behavior of clamped–clamped beam in linear and nonlinear operating conditions can be performed on a second test case. A doubly clamped beam with length *L*= 60 mm, width *w*= 26 mm, thickness *h*=0.3 mm, Young's modulus *E*=160000 MPa and Poisson's coefficient ν=0.3 was analyzed. Actually it exhibits the same stiffness of cantilever beam described in Table 1 and frequency of the first vibration mode is 51.33 Hz.

Analysis of static behavior of this test case is shown in Fig.7. A first solution was found without considering the electromechanical coupling, but only the deflection of beam under a

mechanical concentrated load, being applied to the middle span. In case of two clamps, axial–flexural coupling occurs, thus requiring to resort to the second order theory. By converse in case of one end simply guided along the line axis, without constraining the axial displacement, linear theory is sufficient to describe the characteristic curve of force–vs–flexural displacement. As Fig.7 shows difference is evident, even for low values of force, in case of ideally perfect clamps.

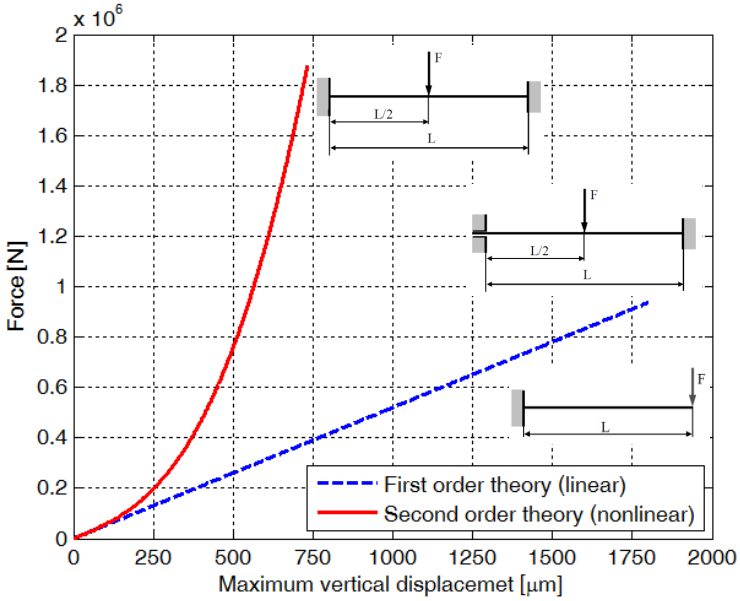

Figure 7: Comparison between linear and geometrically nonlinear behaviors of a doubly clamped beam.

4.2 Role of constraint compliance on the stiffening effect

As Fig.7 points out the two extreme conditions are corresponding to clamped–free and clamped–clamped configuration, respectively. If it is assumed that clamps have an intrinsic compliance, i.e, their inhibition of the axial displacement of beam is moderated by a local axial stiffness k_0, characteristic curve of Fig.7 changes like in Fig.8.

It is remarkable that stiffening effect introduces in the frequency response of system a clear nonlinearity, which is evidenced by the so–called jump of the curve close to the apparent resonance of the dynamic system (as nonlinear resonance concept is not applicable). This effect has two relevant consequences for the energy harvesting purpose. A first is that amplitude of response is fairly high not only in correspondence of a narrow range of frequency values, like in linear systems just close to resonance. A second issue is that above a defined frequency system response is almost filtered, which might be useful to prevent a unforeseen failure of the device. Moreover, the slope of the amplitude curve is regulated by the constraint compliance and dependence on the frequency is almost linear. Obviously the stiffening effect increases the frequency at which amplitude appears to be maximum, before jumping down in the curve.

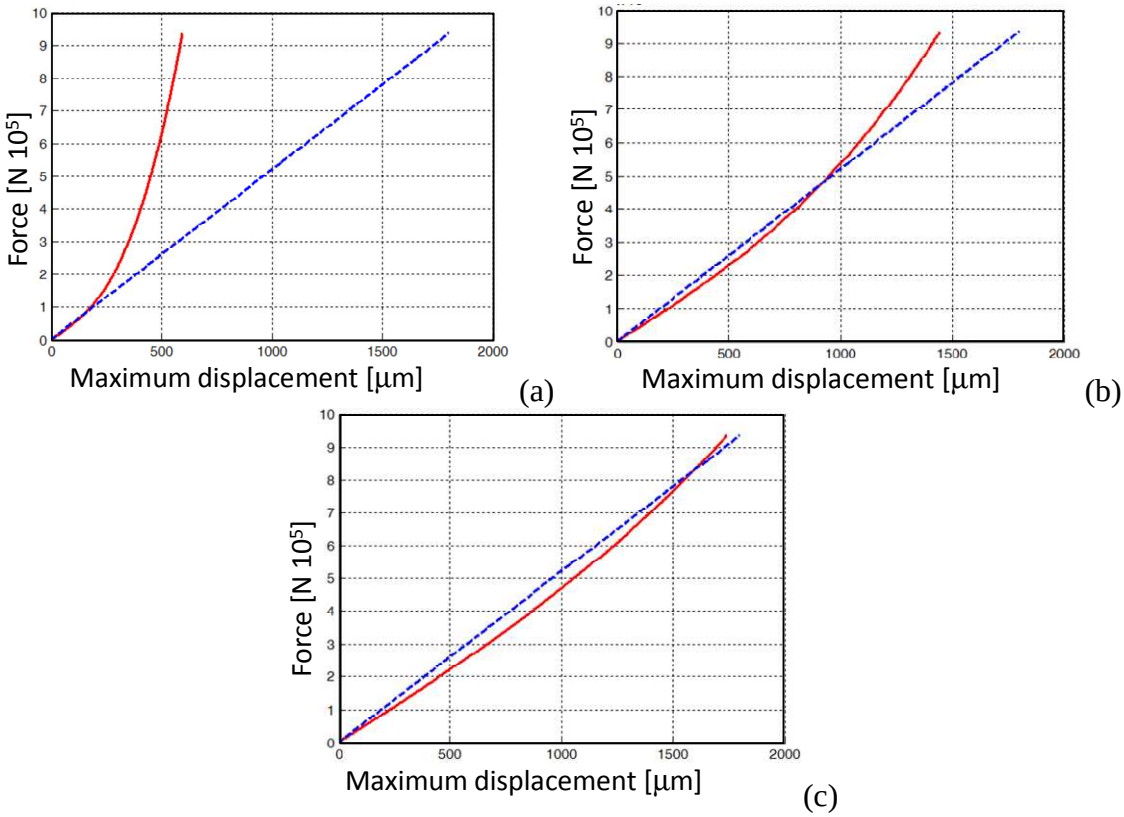

Figure 8: Role of constraint compliance on the geometric nonlinearity of beam: (a) infinitely rigid constraint (b) k_0= 1.53e+005 N/m - high stiffness of clamp (c) k_0= 4.94e+004 N/m - moderate stiffness of clamp.

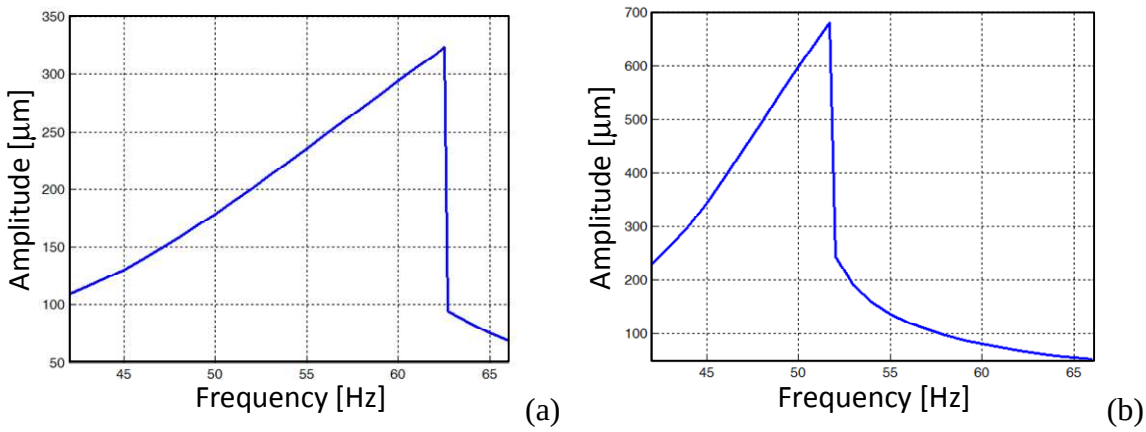

Figure 9: Role of constraint compliance on the nonlinear dynamic response of beam: (a) infinitely rigid constraint (b) moderate stiffness of clamp

5 TOWARDS DESIGN CRITERIA FOR ELECTRETS–BASED ENERGY HARVESTER

5.1 Configuration with one slide

To identify some practical criteria for design from the above investigation, solution for the electromechanical coupled system was analyzed. As a matter of facts, if gap is fairly large the power conversion tends to be lower. Nevertheless, a configuration like in Fig.7 with only a

perfect clamp and the other one allowing the axial displacement (to be referred to as slide) can improve the efficiency of conversion. If simulation is run in case of the first test case and cantilever–based configuration is compared to the clamped–slide layout it can be appreciated that a slight improvement is found. If numerical data are the same for both the configurations, i.e. V=1400 V, d=127 mm, R=300 MΩ, but gap is increased up to g=1 mm, results are those of Fig.10. Damping ratio was set at ζ=0.025, exciting frequency was ω=50 Hz and acceleration amplitude $\ddot{y}_0$=4.5 m/s^2.

Results point out in Fig.10 that excitation basically acts in the same way on the dynamic response of beam, in terms of maximum displacement of tip mass. However, simulation shows that a slight rotation of tip mass in case of cantilever allows to have a slightly less effective coupling. Output voltage is larger in case of clamp and slide, because tip mass is kept with surface aligned with the lower electrode, thus exploiting better the gap between electrodes. In this case it is worthy noticing that first order theory was sufficient for the second configuration, since one clamp allows axial displacement. Stiffening effect with perfect clamps requires to resort to second order theory. For the same inputs of above mentioned cases, it can be immediately appreciated how much the dynamic response is lower, because of the beam stretching (Fig.11).

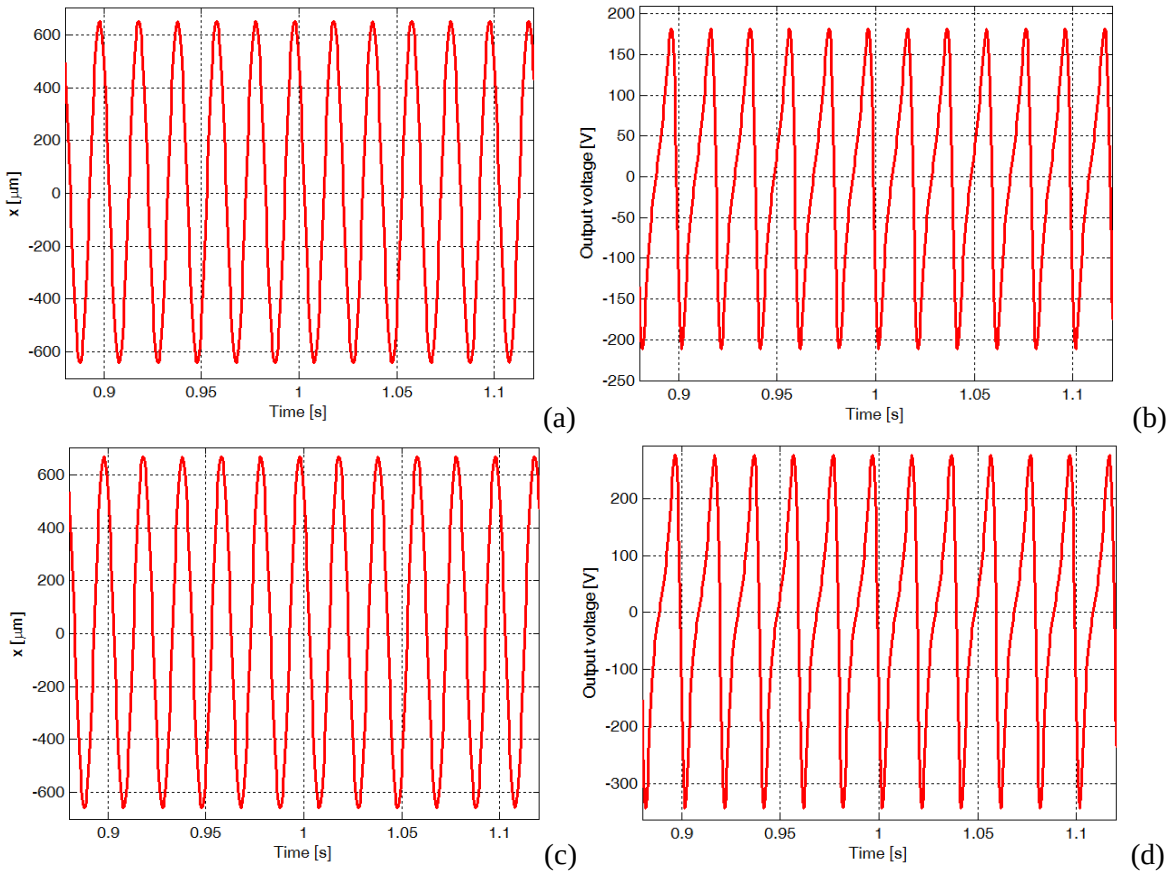

Figure 10: Comparison of performance between (a,b) cantilever and (c,d) clamped–slide configurations.

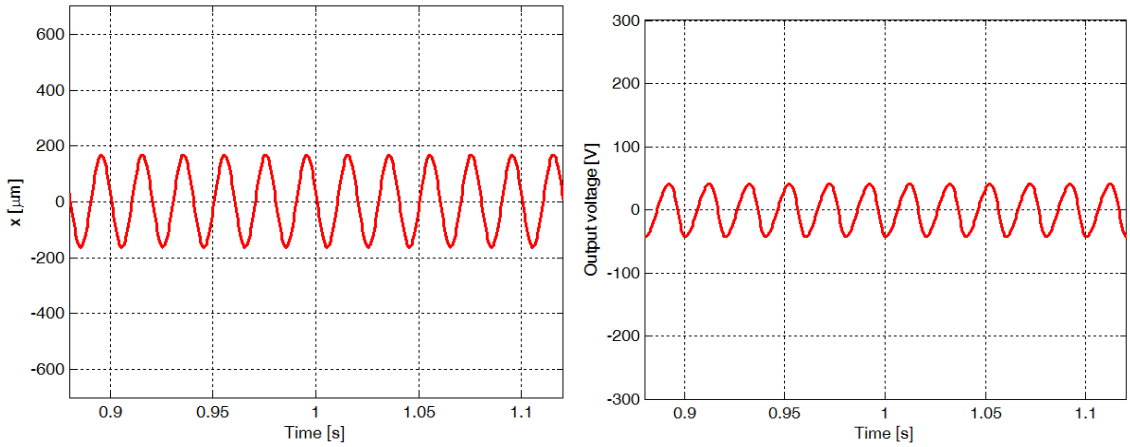

Figure 11: Performance of clamped–clamped beam with same inputs of cases in Fig.10.

5.2 Configuration with double clamps

To fit the need of providing a device fairly sensitive to a wide range of frequency actually geometric nonlinearity may help. If clamped–slide and clamped–clamped beams are compared in terms of dynamic response in the frequency domain, it can be clearly appreciated a significant difference in Fig.12, where results were plotted within the range of variation of voltage described in above Fig.10.

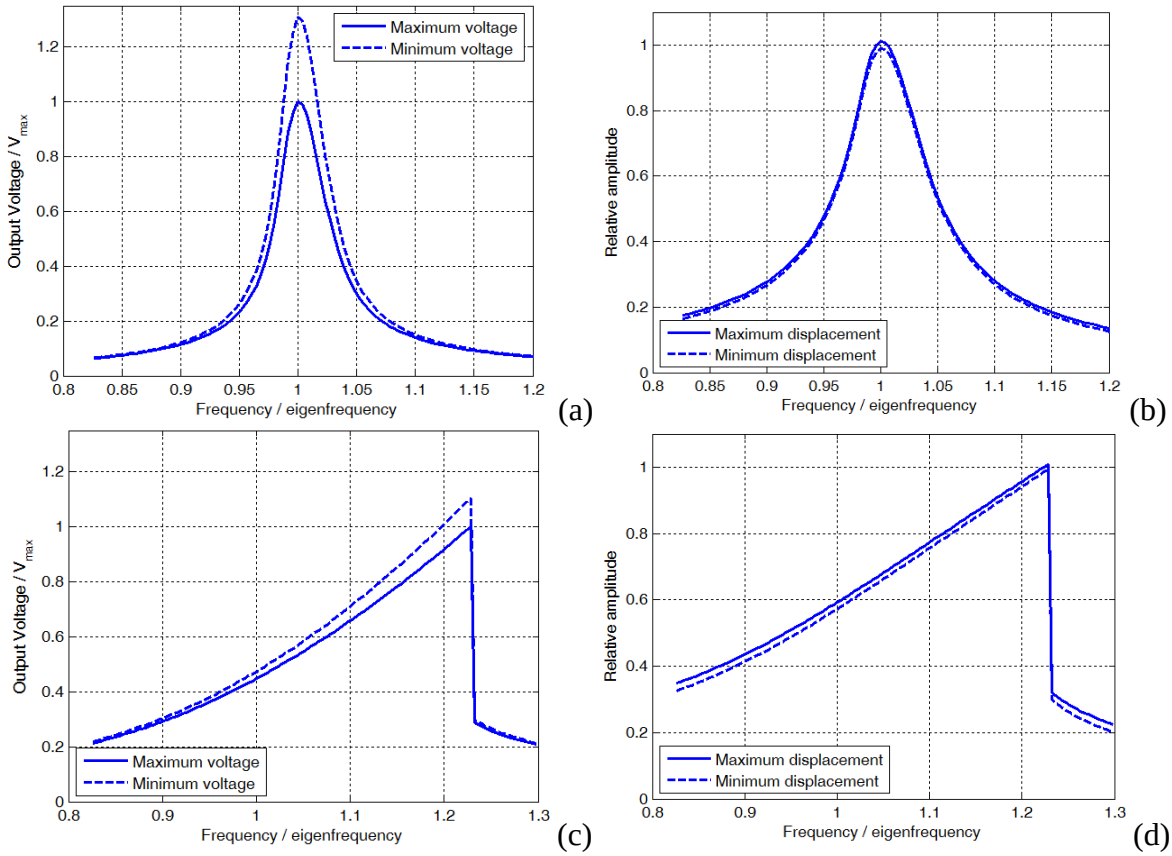

Figure 12: Frequency response of (a,b) clamped–slide and (c,d) clamped–clamped beam configurations.

As it was previously remarked in Fig.12(c,d) the nonlinearity is exploited to have an amplitude variable with frequency, almost linearly. This effect is due to the curved backbone of the path in Fig.12(c,d). In linear system response curve is almost symmetry with respect to so–called backbone, i.e. a symmetry axis which could be plotted along the vertical direction at resonance. In nonlinear system with stiffening effect as amplitude grows up, frequency increases because of the higher stiffness. Therefore peak of resonance moves on right side of the diagram, thus creating a superposition of numerical solution with the lower path of the curve. System naturally tends to reach the solution with associated lower energy consumption and apparently it suddenly jumps down from the peak to a very low level of amplitude. According to Fig.11 and Fig.9(b) a key issue of design might be assessing a suitable value for constraint compliance to find a compromise between the amplitude of dynamic response and the narrow frequency range in which it can be exploited in linear system.

5.3 Optimization

Above analyzed configurations based on clamp–slide and clamped–clamped constraints show some weakness. Linear system provides a narrow range of frequency to usefully operate the energy harvester, the nonlinear system with larger range unfortunately provides a weaker dynamic response in terms of amplitude.

A possible solution could be resorting, like in case of some RF–MEMS [18], to a variable constrained configuration as depicted in Fig.13. In practice, supports are positioned below the deformable electrode at a certain distance. Therefore, effects of clamps when beam access to contact with supports looks like more compliant, because of the portion of beam supported between the clamp and the middle part of the structure. Performance is described in Fig.14. It is pointed out how the amplitude of dynamic response is kept almost maximum within a wider range of frequency, while deflection is fairly large in a first step of bending.

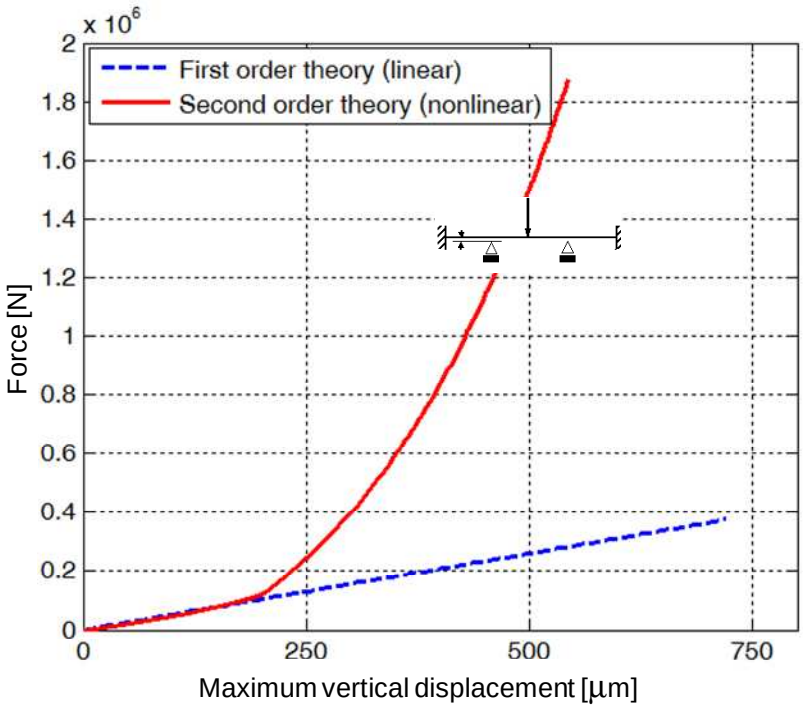

Figure 13: Characteristic curve of clamped–clamped beam configuration with supports.

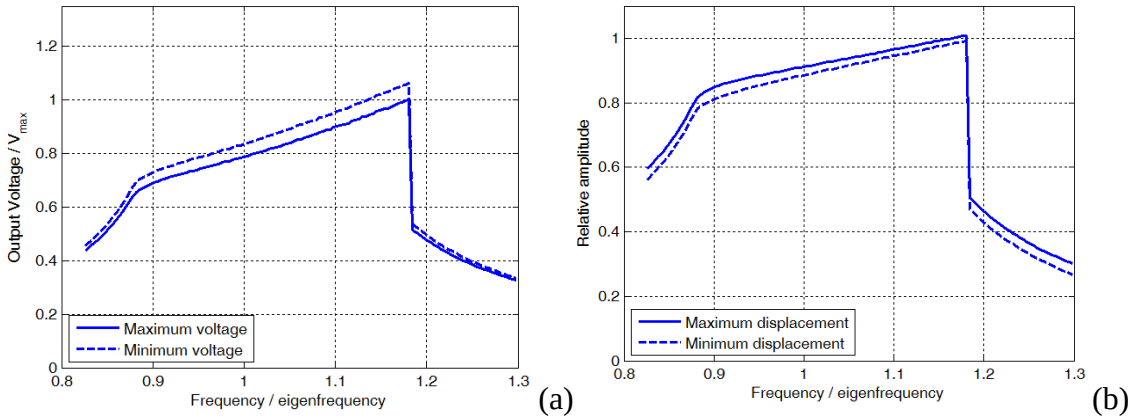

Figure 14: Frequency response of clamped–clamped beam configuration with supports.

This layout may overcome some problems evidenced in [14], where the authors introduced some nonlinear springs espressively microfabricated to exploit some benefits of nonlinear behaviour of structural elements of energy harvesting.

6 CONCLUSION

The literature claim that a main benefit of electret materials applied to microtechnology and energy harvesters is making possible to provide a local and autonomous power supply for miniaturized devices, based on capacitive systems, where a bias voltage is required to operate the energy conversion. Nevertheless, performance of those materials is still considered somehow insufficient to have a relevant technological impact. Actually, it can be noticed that effectiveness of electrets–based system does not depend uniquely upon the coupling coefficients of such smart material, but even on the dynamic behaviour exploited for converting energy. In this paper the case of energy harveters based on flexible beams was analyzed. A first contribution consists of focusing on the nonlinear behavior exhibited by the clamped–clamped configuration, because of mechanical coupling between axial and flexural behavior. Stiffening effect associated to beam strecthing actually might reduce the peak of amplitude reached in dynamic behavior, but range of frequency for which the amplitude of vibration mode of beam is fairly high is increased. As a consequence a key issue of design are compliance and configuration of supports. If beam is supported by compliant clamps, with a defined stiffness, a compromise between the best peak of dynamic response achievable and frequency bandwidth in which it is kept almost maximum can be found. Nonlinear behaviour might help in assuring the best conversion over a suitable range of uncertainty concerning the frequency of excitation. Obviously design must assure the suitable level of reliability against structural damage. A preliminary optimization was proposed, being based on a solution in which additional supports are used to excite the nonlinear response, above a certain amplitude of vibration. Future work could investigate some practical issues about the proposed solution on small prototypes of energy harvester. However, a slight benefit in efficiency was demostrated, despite of low coupling effect provided by some electret material.

REFERENCES

[1] S. Wilson et alii, New materials for microscale sensors and actuators – an engineering review, *Materials Science and Engineering*, **R56**, 1–129, 2007.

[2] G. Evreinov, R. Raisamo, One–directional position–sensitive force transducer based on EMFi, *Sensors and Actuators A*, **123–124**, 204–209, 2005.

[3] P. Mitcheson, E. Yeatman, G. K. Rao, A. S. Holmes, T. C. Green, Energy Harvesting from human and machine motion for wireless electronic devices, *Proceedings of the IEEE*, **96(9)**, 1457–1486, 2008.

[4] S. Boisseau, G. Despesse, B. A. Seddik, Electrostatic conversion for vibration energy harvesting, in *Small–Scale Energy Harvesting*, Intech, 2012.

[5] T. Sterken, P. Fiorini, K. Baert, K. Puers, G. Borghs, An electrets–based electrostatic–generator, in Proc. 12th Int. Conf. Solid State Sensors, Actuators Microsystems (Transducers), Boston, MA, Jun. 2003, pp. 1291–1294.

[6] H. Okamoto,T. Suzuki, K. Mori, Z. Cao, T. Onuki, H. Kuwano, The advantages and potential of electrets–based vibration–driven micro energy harvesters, *Int. J. Energy Res.*, **33**, 1180–1190, 2009.

[7] M. Mizuno, D.G. Chetwynd, Investigation of a resonance microgenerator, *J. Micromech. Microeng.*, **13**, pp. 209–216, 2003.

[8] M. Paajanen, H. Vaklimakki, J. Lekkala, Modelling the electromechanical film (EMFi), *Journal of Electrostatics*, **48**,193–204, 2000.

[9] M. Paajanen, J. Lekkala, K. Kirjavainen, ElectroMechanical Film_EMFi — a new multipurpose electret material, *Sensors and Actuators*, **84**, 95–102, 2000.

[10] Q. Deng, L. Liu, P. Sharma, Electrets in soft materials: Nonlinearity, size effects, and giant electromechanical coupling, *Physical Review E*, **90**, 0126031–7, 2014.

[11] P. Bettini, E. Brusa, M. Munteanu, R. Specogna, F. Trevisan, Innovative numerical methods for nonlinear MEMS: the non incremental FEM vs. the Discrete Geometric Approach, *Computer Modelling for Engineering and Sciences (CMES)*, **33(3)**, 215–242, 2008.

[12] S. Boisseau et al., Cantilever–based energy harvesters, *Smart Mater. Struct.*, **20** (105013), 2011.

[13] Y. Chiu, Y-C. Lee, Flat and robust out–of–plane vibrational electret energy harvester, *J. Micromech. Microeng.* **23**, 015012–8pp, 2013.

[14] D. Miki, M. Honzumi, Y. Suzuki, N. Kasagi, Large amplitude MEMS electrect generator with nonlinear spring, *Proc. IEEE*, pp.176–179, 2013, ISBN-978-1-4244-5764-9.

[15] Y. Suzuki, D. Miki, M. Edamoto, M. Honzumi, A MEMS electret generator with electrostatic levitation for vibration-driven energy-harvesting applications, *J. Micromech. Microeng.* **20**, 104002–8pp**,** 2010.

[16] E. Brusa, Dynamics of mechatronic systems at microscale, in *Microsystem Mechanical Design*, CISM Lectures Series, 478, Springer Verlag, Wien, 2006, pp.57–80.

[17] O.C. Zienlkiewicz, R.L. Taylor, The Finite Element Method, Fifth edition, Butterworth-Heinemann, 2004.

[18] S. Lucyszyn, Advanced RF MEMS, Cambridge University Press, Cambridge, UK, 2010.